Azocarbazole Polymethacrylates as Single-Component Electrooptic Materials

Christopher Barrett,[†,‡] Biswajit Choudhury,[†] Almeria Natansohn,*,[†] and Paul Rochon[§]

Department of Chemistry, Queen's University, Kingston, Ontario, Canada K7L 3N6, and Department of Physics, Royal Military College, Kingston, Ontario, Canada K7K 5L0

Received February 3, 1998; Revised Manuscript Received May 22, 1998

ABSTRACT: A series of amorphous azobenzene and carbazole-containing polymers was prepared, which incorporates both electrooptic activity and photoconductivity into a single multifunctional structural unit. The polymers were cast as thin films and were shown to be suitable for photoinducing birefringence reversibly with polarized light, as well as for the inscription of photorefractive diffraction gratings after electric field poling. Since the polymer series encompasses a range of spacer lengths (from 3 to 10 methylene groups) between the multifunctional side chains and the polymer backbone, these materials are suitable for study of the influence of chromophore mobility on these optical phenomena. The extent of orientational order which could be photoinduced in the films was found to decrease with increasing spacer length, as did the photoconductivity and the photorefractive two-beam optical coupling gain. In thin films of polymers with the highest glass transition temperature, a birefringence of 0.065 could be photoinduced, with a time constant of <0.8 s. A two-beam optical gain of 0.024 μm^{-1} was also demonstrated in films of the polymer with the highest glass transition temperature, although this gain was exceeded by absorption losses.

Introduction

Polymers which incorporate both photoconductive and electrooptic functionalities can be regarded as suitable materials for a wide range of optical and electrooptic applications. If the electrooptic (EO) chromophores are based on an azobenzene structure, these groups can be preferentially oriented with a polarized laser for reversible optical storage[1,2] and for the inscription of channel waveguides.[3,4] In addition, thin films of these azobenzene-based chromophores have been shown to be suitable for the laser inscription of high efficiency surface relief diffraction gratings.[5,6] Systems which can be poled and possess both photoconductivity and a sufficient EO response can also be suitable for the inscription of photorefractive (PR) gratings.[7−9] With diffraction efficiencies which can approach 100%[10] and grating inscription times which can be as brief as 60 ms,[11] poled photorefractive polymers have now begun to perform competitively with traditional inorganic crystals, and they possess some advantages such as lower cost, greater versatility, and relative ease of preparation and processing.

It is usually an advantage with multifunctional polymers if the individual components are incorporated in as high a concentration as possible, both for optimal performance and for increased efficiency. Hence, there has been much interest in materials which combine the photoconductive and EO components into a single multifunctional structural unit.[12−16] It can also be a distinct advantage (for optical purity and for thermal stability) if this single multifunctional unit is bound to the polymer backbone, and for this reason there has been recent interest in fully functionalized multicomponent polymer systems.[17,18]

In a previous report,[17] thin films of a novel side chain azobenzene−carbazole polymer were shown to be suitable materials for reversibly photoinducing birefringence, for inscribing high efficiency surface relief gratings, and for storage of a photorefractive grating. This azocarbazole single-component multifunctional side group was bound to a methacrylate backbone with a short ethylene spacer. While this produced a high (>165 °C) glass transition temperature (T_g) material which exhibited high thermal stability, the mobility of the side chains was necessarily limited. Since all of the optical phenomena reported require mobility for optimal performance, the material with the highest T_g is not necessarily optimal, as there is a trade off between ease of induced orientation and retention of induced order over time due to thermal relaxations.

In this paper the preparation and optical characterization of a series of multifunctional single-component polymers based on this azocarbazole structure is described, where the distance between the chromophore and the methacrylate main chain is systematically increased by the number of methylene groups in the spacer (from 3 to 10). Photoinduced birefringence and photorefractivity are studied with polymers of this series as a function of their structure.

Experimental Section

Proton spectra were recorded on a Bruker AC−F 200 NMR spectrometer. The molecular weight of the polymers (relative to polystyrene) was determined with a Waters Associates Liquid Chromatograph equipped with μ-styragel columns and a R401 differential refractometer. The glass transition temperatures (T_g) were determined with a Mettler TA 3000 thermal analysis system equipped with TC10A TA processor and DSC30 head. Cast films were determined to be amorphous by polarized microscopy using a Nikon Labophot-2 microscope equipped with a Leitz heating stage and the electronic spectra of the films were recorded with a Shimadzu TR-280 UV−visible spectrophotometer. The preparation of the materials is summarized in Scheme 1.

[†] Queen's University.
[‡] Current address: Department of Materials Science and Engineering, MIT, Cambridge, MA 02139.
[§] Royal Military College.

Scheme 1
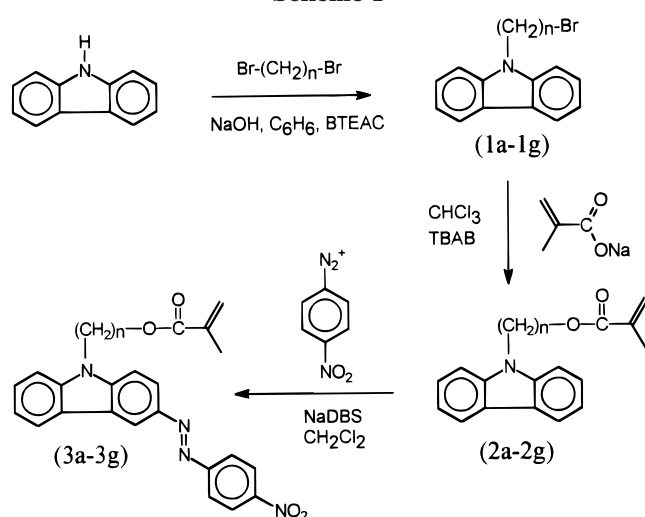
Preparation of *N*-[ω-(Bromoalkyl)]carbazoles (1a–g).

To a mixture of carbazole (5.0 g, 30 mmol), benzene (15 mL), benzyltriethylammonium chloride (BTEAC) (250 mg), and aqueous (50%) sodium hydroxide solution (15 mL), an excess amount (greater than 10-fold equivalent to carbazole) of alkyl dibromide was added under stirring.

N*-(3′-Bromopropyl)carbazole (1a). Yield: 91%. Mp: 124 °C. ^{1}H NMR (CDCl$_3$): δ 2.12 (m, 2H), 3.62 (t, 2H), 4.48 (t, 2H), 7.20–7.30 (m, 2H), 7.45 (m, 4H), 8.09 (m, 2H).

N*-(4′-Bromobutyl)carbazole (1b). Yield: 88%. Mp: 107 °C. ^{1}H NMR (CDCl$_3$): δ 1.80–2.20 (m, 4H), 3.37 (t, 2H), 4.34 (t, 2H), 7.18–7.29 (m, 2H), 7.46–7.51 (m, 4H), 8.10 (m, 2H).

N*-(5′-Bromopentyl)carbazole (1c). Yield: 76%. Mp: 72 °C. ^{1}H NMR (CDCl$_3$): δ 1.52 (m, 4H), 1.86 (m, 4H), 3.34 (t, 2H), 4.27 (t, 2H), 7.18–7.31 (m, 2H), 7.33–7.51 (m, 4H), 8.11 (m, 2H).

N*-(6′-Bromohexyl)carbazole (1d). Yield: 70%. Mp: 58 °C. ^{1}H NMR (CDCl$_3$): δ 1.31–1.55 (m, 4H), 1.73–1.95 (m, 4H), 3.35 (t, 2H), 4.30 (t, 2H), 7.17–7.26 (m, 2H), 7.32–7.50 (m, 4H), 8.95 (m, 2H).

N*-(8′-Bromooctyl)carbazole (1e). Yield: 66%. ^{1}H NMR (CDCl$_3$): δ 1.20–1.46 (m, 8H), 1.75–1.98 (m, 4H), 3.38 (t, 2H), 4.31 (t, 2H), 7.21–7.28 (m, 2H), 7.38–7.55 (m, 4H), 8.12 (m, 2H).

N*-(9′-Bromononyl)carbazole (1f). Yield: 65%. ^{1}H NMR (CDCl$_3$): δ 1.20–1.55 (m, 10H), 1.76–1.95 (m, 4H), 3.39 (t, 2H), 4.26 (t, 2H), 7.20–7.35 (m, 2H), 7.36–7.57 (m, 4H), 8.13 (m, 2H).

N*-(10′-Bromodecyl)carbazole (1g). Yield: 78%. ^{1}H NMR (CDCl$_3$): δ 1.18–1.26 (m, 12H), 1.72–1.79 (m, 4H), 3.32 (t, 2H), 4.28 (t, 2H), 7.16–7.40 (m, 6H), 8.03 (d, 2H).

Preparation of *N*-[ω-(Methyacryloxy)alkyl]carbazoles (2a–g).

A mixture of N–(ω′-bromoalkyl) carbazole (32.1 mmol) in chloroform (75 mL), tetrabutylammonium bromide (2.1 g, 7.5 mmol) and an aqueous solution (25 mL) of sodium methacrylate (14.0 g, 129.1 mmol) containing a trace amount of hydroquinone was stirred at 55 °C for 48 h. The organic layer was extracted with chloroform, dried over anhydrous Na$_2$SO$_4$. The solvent was removed under reduced pressure, and the residue was purified by silica gel column chromatography. The pure products were obtained by removing the solvent under reduced pressure.

N*-[3′-(Methacryloxy)propyl]carbazole (2a). Yield: 72%. Mp: 45 °C. ^{1}H NMR (CDCl$_3$): δ 1.93 (s, 3H), 2.24 (q, 2H), 4.15 (t, 2H), 4.43 (t, 2H), 5.56 (m, 1H), 6.12 (m, 1H), 7.19–7.28 (m, 2H), 7.37–7.51 (m, 4H), 8.10 (d, 2H).

N*-[4′-(Methacryloxy)butyl]carbazole (2b). Yield: 86%. ^{1}H NMR (CDCl$_3$): δ 1.67–1.81 (m, 2H), 1.92–2.06 (m, 5H), 4.16 (t, 2H), 4.35 (t, 2H), 5.54 (m, 1H), 6.06 (m, 1H), 7.18–7.29 (m, 2H), 7.36–7.50 (m, 4H), 8.12 (d, 2H).

N*-[5′-(Methacryloxy)pentyl]carbazole (2c). Yield: 78%. ^{1}H NMR (CDCl$_3$): δ 1.39–1.56 (m, 2H), 1.63–1.77 (m, 2H), 1.85–2.01 (5H), 4.10 (t, 2H), 4.31 (t, 2H), 5.51 (m, 1H), 6.03 (m, 1H), 7.16–7.29 (m, 2H), 7.35–7.54 (m, 4H), 8.10 (d,2H).

N*-[6′-(Methacryloxy)hexyl]carbazole (2d). Yield: 75%. ^{1}H NMR (CDCl$_3$): δ 1.38–1.45 (m, 4H), 1.67 (m, 2H), 1.84–1.94 (m, 5H), 4.11 (t, 2H), 4.30 (t, 2H), 5.54 (m, 1H), 6.09 (m, 1H), 7.17–7.31 (m, 2H), 7.38–7.52 (m, 4H), 8.12 (m, 2H).

N*-[8′-(Methacryloxy)octyl]carbazole (2e). Yield: 62%. ^{1}H NMR (CDCl$_3$): δ 1.33 (m, 8H), 1.58–1.68 (m, 2H), 1.77–1.96 (m, 5H), 4.14 (t, 2H), 4.29 (t, 2H), 5.56 (m, 1H), 6.12 (m, 1H), 7.22–7.29 (m, 2H), 7.37–7.52 (m, 4H), 8.13 (d, 2H).

N*-[9′-(Methacryloxy)nonyl]carbazole (2f). Yield: 61%. ^{1}H NMR (CDCl$_3$): δ 1.34 (m, 10H), 1.62–1.75 (m, 2H), 1.81–2.01 (m, 2H), 4.17 (t, 2H), 4.30 (t, 2H), 5.58 (m, 1H), 6.17 (m, 1H), 7.20–7.33 (m, 2H), 7.35–7.56 (m, 4H), 8.15 (d, 2H).

N*-[10′-(Methacryloxy)decyl]carbazole (2g). Yield: 62%. ^{1}H NMR (CDCl$_3$): δ 1.22 (m, 12H), 1.57 (t, 2H), 1.80 (t, 2H), 1.86 (s, 3H), 4.05 (t, 2H), 4.23 (t, 2H), 5.46 (t, 1H), 6.02 (t, 1H), 7.15 (m, 2H), 7.36 (m, 4H), 8.03 (d, 2H).

Preparation of 4″-Nitrophenyl-3-[*N*-[ω′-(methacryloxy)-alkyl]]carbazolyl Diazenes (3a–g).

4-Nitroaniline (2.0 g, 14 mmol) and concentrated HCl (8 mL) were mixed in 200 mL of water. The mixture was cooled in an ice bath, and a solution of sodium nitrite (1.2 g, 17 mmol) in water (10 mL) was added slowly to the 4-nitroaniline solution. The mixture was allowed to stir in the ice bath for 30 min, while the yellow solution became colorless. Sodium dodecylbenzenesulfonate (NaDBS) (1.0 g) was then added to the mixture, and the mixture was stirred vigorously at 3 °C for 15 min. N-[ω′-(methacryloxy)-alkyl]carbazole (30 mmol) dissolved in 225 mL of dichloromethane was dropwise added to the reaction mixture. The reactant mixture was stirred vigorously at room temperature for 48 h. The product was extracted with CH$_2$Cl$_2$ and dried over anhydrous Na$_2$SO$_4$. The solvent was removed under reduced pressure. The residue was purified by silica gel column chromatography. Pure products were obtained after removing the solvent under reduced pressure.

4″-Nitrophenyl-3-[*N*-[3′-(methacryloxy)propyl]]carbazolyl Diazene (3a). Yield: 10%. Mp: 78 °C. ^{1}H NMR (CDCl$_3$): δ 1.96 (s, 3H), 2.15–2.37 (m, 2H), 4.17 (t, 2H), 4.49 (t, 2H), 5.61 (m, 1H), 6.12 (m, 1H), 7.25–7.35 (m, 1H), 7.41–7.56 (m, 3H), 8.12–8.19 (m, 2H), 8.33–8.40 (m, 2H), 8.73 (d, 1H).

4″-Nitrophenyl-3-[*N*-[4′-(methacryloxy)butyl]]carbazolyl Diazene (3b). Yield: 12%. Mp: 75 °C. ^{1}H NMR (CDCl$_3$): δ 1.70–1.84 (m, 2H), 1.90–2.06 (m, 5H), 4.18 (t, 2H), 4.40 (t, 2H), 5.54 (m, 1H), 6.05 (m, 1H), 7.21–7.56 (m, 4H), 8.00–8.19 (m, 4H), 8.33–8.38 (m, 2H), 8.73 (d, 2H).

4″-Nitrophenyl-3-[*N*-[5′-(methacryloxy)pentyl]]carbazolyl Diazene (3c). Yield: 11%. Mp: 72 °C. ^{1}H NMR (CDCl$_3$): δ 1.40–1.554 (m, 2H), 1.65–1.79 (m, 2H), 1.87–2.10 (m, 5H), 4.11 (t, 2H), 4.37 (t, 2H), 5.50 (m, 1H), 6.01 (m, 1H), 7.27–7.56 (m, 4H), 8.01–8.19 (m, 4H), 8.35–8.40 (m, 2H), 8.74 (d, 2H).

4″-Nitrophenyl-3-[*N*-[6′-(methacryloxy)hexyl]]carbazolyl Diazene (3d). Yield: 14%. Mp: 70 °C. ^{1}H NMR (CDCl$_3$): δ 1.41–1.48 (m, 4H), 1.58–1.69 (m, 2H), 1.82–1.89 (m, 5H), 4.12 (t, 2H), 4.37 (t, 2H), 5.54 (m, 1H), 6.08 (m, 1H), 7.29–7.58 (m, 4H), 8.03–8.21 (m, 4H), 8.36–8.43 (m, 2H), 8.75 (d, 2H).

4″-Nitrophenyl-3-[*N*-[8′-(methacryloxy)octyl]]carbazolyl Diazene (3e). Yield: 12%. Mp: 69 °C. ^{1}H NMR (CDCl$_3$): δ 1.25 (m, 8H), 1.48–1.62 (m, 2H), 1.76–1.90 (m, 5H), 4.04 (t, 2H), 4.26 (t, 2H), 5.45 (m, 1H), 6.00 (m, 1H), 7.21–7.50 (m, 4H), 7.89–8.12 (m, 4H), 8.25–8.32 (m, 2H), 8.66 (d, 2H).

4″-Nitrophenyl-3-[*N*-[9′-(methacryloxy)nonyl]]carbazolyl Diazene (3f). Yield: 9%. Mp: 67 °C. ^{1}H NMR (CDCl$_3$): δ 1.24 (m, 10H), 1.46–1.63 (m, 5H), 4.09 (t, 2H), 4.28 (t, 2H), 5.42 (m, 1H), 6.01 (m, 1H), 7.21–7.49 (m, 4H), 7.87–8.09 (m, 4H), 8.21–8.30 (m, 2H), 8.68 (d, 2H).

4″-Nitrophenyl-3-[*N*-[10′-(methacryloxy)decyl]]carbazolyl Diazene (3g). Yield: 16%. Mp: 79 °C. ^{1}H NMR (CDCl$_3$): δ 1.28 (m, 12H), 1.56 (t, 2H), 1.93 (m, 5H), 4.12 (t,

2H), 4.36 (t, 2H), 5.53 (s, 1H), 6.08 (s, 1H), 7.26 (m, 2H), 7.48 (m, 2H), 8.06 (d, 2H), 8.12 (m, 2H), 8.40 (d, 2H), 8.77 (d, 1H).

Polymerization of Monomers (3a−g): Preparation of Poly[nitrophenyl-[3-[*N*-[*ω*′-(methacryloxy)alkyl]]carbazolyl diazene]. The polymerization for all the monomers was carried out in 1,2-dichlorobenzene with 10% 2,2′-azobisisobutyronitrile (AIBN) as initiator. The reaction solution was purged with argon for 30 min and sealed. The monomer was allowed to polymerize under argon at 60 °C for 2 days. The polymerization was stopped by precipitating the reaction solution in ethanol. The polymer was obtained by filtration and purified by reprecipitation the polymer solution from THF into ethanol and dried under vacuum. The preparation of the azocarbazole polymer with an ethylene spacer was published previously.[17]

Sample Preparation. The *n*-variable spacer poly(azocarbazole) (PAC-*n*) polymers used in this study were cast as films onto transparent substrates, either cleaned glass microscope slides, or indium−tin−oxide- (ITO-) coated glass when an electrically conductive substrate was required. For studies of photoinduced orientation, spin-cast films on glass were prepared, for determination of photoconductivity and poling dynamics the polymer was "sandwiched" between two ITO plates so that an electric field could be applied normal to the substrate, and for optical gain coupling polymer cells were cast in etched channels of ITO on glass, so that an electric field could be applied parallel to the substrate.

To produce thin films, the polymers were dissolved in tetrahydrofuran (THF), spin-cast onto clean glass substrates, and heated to $T_g + 10$ °C to yield dry amorphous films of good optical quality and of thickness between 200 and 400 nm.

For EO sandwich samples, ITO-coated glass substrates were masked with tape, and the exposed ITO was dissolved in a concentrated HCl/HNO₃ acid bath to remove all of the ITO except for a 2 mm-wide strip centered on the substrate, and the sample was then cleaned with distilled water and methanol. Dry powdered polymer was deposited on the ITO strip, and a second etched substrate was placed on top of the first, inverted, and rotated such that the two ITO strips were adjacent to the polymer with an area of intersection of ∼4 mm². The samples were heated to a temperature of $T_g + 30°$ for 2 h while applying a force of ∼100 g/cm² on the top plate and then cooled slowly to room temperature over 4 h. This yielded polymer sandwiches of good optical quality, of a thickness between 1 and 10 μm, and with electric plates on both sides of the film which could be addressed to apply a field across the polymer normal to the plane of the film. Film thickness of the sandwiches was determined by optical absorbance, relative to the corresponding thin film where thickness could be determined directly by interferometry.

To produce polymer EO cells, ITO-coated glass substrates were similarly acid-etched to yield ITO strips running the width of the substrate, with a width of 4 mm, and a narrow (∼150 μm) channel etched midway. Polymer dissolved in THF was deposited into this 0.15 mm × 4 mm cell and slow-evaporated to yield a laterally-ITO-bound electooptic polymer cell of good optical quality with a thickness between 600 and 1200 nm. Electrodes were attached to the exposed ends of the ITO fingers so that an electric field could be applied across the polymer film parallel to the plane of the substrate. Thickness was determined by interferometry of the polymer film directly adjacent to the cell, and the cell width was determined by optical microscopy with a linearly-ruled distance scale. The three types of cast films are depicted in Figure 1.

Optical Characterization. Induced order in the polymer samples was measured by photoinducing birefringence similar to methods described previously,[1] where a 633 nm probe beam was attenuated to 0.01 mW, linearly polarized 45° off-axis, and introduced normal to the polymer thin films which were placed between crossed polarizers oriented along and against the axis of probe beam polarization. The intensity of the light passing through crossed polarizers and into a photomultiplier tube was then monitored over time while birefringence was induced in the sample by a 3 mW pump (or "writing") beam at 488 nm
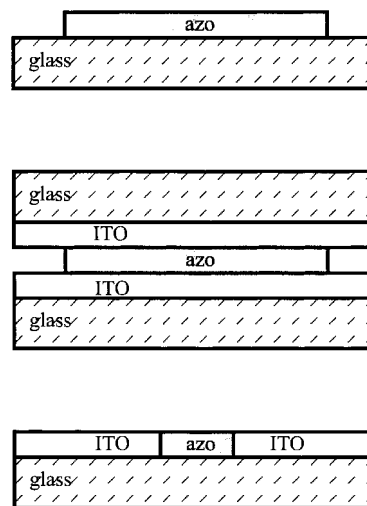

Figure 1. Azocarbazole polymer cast as a thin film (top), an electrooptic sandwich (center), and an electrooptic cell (bottom).

linearly polarized on-axis from an Ar⁺ laser, coincident with the probe beam on the sample. The writing beam polarization could be modulated with a Pockels cell to switch from linear (for writing birefringence) to circular (to erase) polarizations.

Photoconductivity of the PAC-*n* polymer series was determined as described,[19] by measuring the difference between the dark current and that resulting from 2 mW/mm² 633 nm laser irradiation of the sample with a 50 V/μm applied voltage.

Optical characterization of the photorefractive effect was conducted in the red region at 633 nm so as to minimize the competition between PR gratings and birefringence gratings (which are of much lower efficiency when inscribed at 633 nm) and between PR gratings and surface relief gratings (which have not been observed with a 633 nm writing wavelength). To further characterize photorefractivity unambiguously, the PR effect was measured by two-beam optical gain coupling as opposed to PR grating diffraction efficiency, as the PR effect is the only mechanism that could be responsible for asymmetric beam coupling.[7] Electrooptic polymer cells were placed in an oven and heated to $T_g + 20$ °C over 30 min. A DC field of 15 V/μm was then applied for 90 min at this temperature and maintained while the sample was cooled back down to room temperature over a further 90 min before removal. The cells were then immediately placed in an optical setup similar to that described in the literature.[7,20] Two 633 nm *s*-linearly polarized writing beams of equal power at 1.5 mW were focused to ∼200 μm in diameter and coincided in the cell to produce an interference pattern with $2\theta = 46°$. The beams could be selectively removed and introduced with a manual shutter, and the intensity of either beam could be measured with a photodiode and recorded. To measure asymmetric gain or loss, the intensity of one beam was recorded while the second was introduced and removed, and then the same procedure was carried out for the second beam while the first was removed and then reintroduced.

Results and Discussion

The azobenzene-based polymers comprise an eight-member series of poly(azocarbazole) polymers (PAC-*n*), linked to a methacrylate backbone by a spacer of variable length (*n*) from 2 to 10 methylene units. The results of glass transition temperature determination, average MW determination, and optical characterization are shown in Table 1.

It is clear that there does not appear to be a significant difference in the absorbance maxima of the samples, as the λ_{max} values for all samples are contained within a range of 440−450 nm, nor does there appear to be a significant variation in the extinction coefficients. One

**Table 1. Physical and Optical Characteristics of the
PAC-*n* Polymer Series**

n	T_g (°C)	T_{dec} (°C)	MW (g/mol)	λ_{max} (nm)	ϵ_{445} (μm^{-1})	ϵ_{633} (μm^{-1})	Δn	$10^{13}\Phi$ (A/V·cm)
2	167	286	9200	444	3.9	0.27	0.065	2.8
3	127	288	3600	440	3.8	0.26	0.064	2.1
4	99	293	4200	443	4.2	0.29	0.058	2.5
5	88	289	4450	447	3.5	0.24	0.053	2.0
6	81	285	3600	450	3.2	0.22	0.054	1.7
8	70	298	6200	445	3.7	0.26	0.045	2.1
9	69	295	4700	443	3.8	0.26	0.051	1.7
10	65	282	6200	445	3.7	0.26	0.042	1.9

might expect a slight decrease in the extinction coefficients with increasing spacer length, due to a decrease in the relative concentration of the absorbing chromophores across the series, from "dilution" in the bulk with the methylene units. This relative chromophore dilution would be expected to be near 20% from the PAC-2 to the PAC-10 polymer. This trend is consistent with the ϵ data in Table 1, as far as the experimental uncertainty of $\pm 10\%$ (due to the determination of film thickness) allows a comparison. The absence of other apparent trends in the λ_{max}, ϵ_{445}, and ϵ_{633} results suggests that there is not an appreciable variation in the electronic environment of the chromophores across the series and that the azo chromophores can be considered to be in a similar electronic environment for all polymers in the series.

A distinct trend is clear from the T_g values presented in Table 1, as the T_g is depressed by more than 100 deg with the increase in the number of chain spacers from 2 to 10 methylene units. This suggests that there is a substantial increase in the mobility across the series from the PAC-2 to the PAC-10 polymers and that this is most pronounced at short spacer lengths. A difference in T_g of only 5 degrees is observed between the three samples with the longest methylene spacers of $n = 8$, 9, and 10, which is within the experimental uncertainty of T_g determination and the inherent range of the transition itself. These T_g values are in agreement with the characterization results of a similar series of poly-(*n*-methylenecarbazole) photorefractive polymers, where an increase in the length of methylene spacer between a carbazole moiety and methacrylate backbone from 2 to 11 units resulted in a T_g decrease from 148 to 31 °C.[21] In another similar study with main chain carbazole-based polymers,[18] extension of an alkyl chain pendant on the carbazole group (introduced to lower T_g) from 6 to 13 methylene units depressed the T_g to 53 °C from 87 °C.

In examining the dependence on the mobility of optical and electrooptic effects, it would be reasonable to expect that the most pronounced influence would be on the phenomena which involve reorientation of the side groups in the polymer matrix, such as electric field poling and photoinduced birefringence. Once an electrooptic thin film sandwich of azo polymer is brought to T_g, application of an electric field across the film induces poling and aligns the dipoles with the applied electric field, as measured by the birefringence between crossed polarizers while a poling field of 50 V/μm was applied to the samples at T_g + 20 °C. The poling rates for all of the samples appeared to be similar, though low signal-to-noise ratios in these films precluded a quantitative comparison.

A more useful comparison of orientational dynamics across the polymer series can be made at room temper-
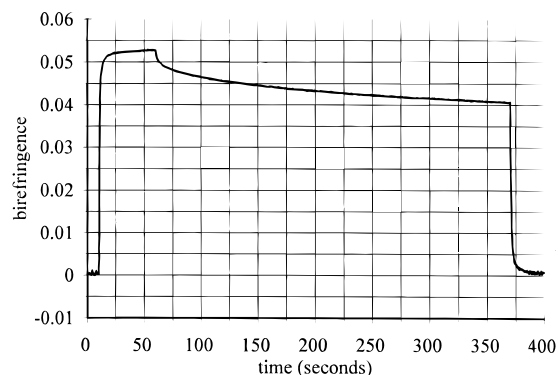
Figure 2. Photoinduced and erased birefringence in a PAC-5 polymer thin film.

ature by photoinducing orientation with a linearly polarized laser, as this technique can induce a high degree of orientational order in all of the samples under the same conditions, and with a high-enough signal-to-noise ratio to collect data of a resolution suitable for curve fitting. Since these experiments were carried out at room temperature, below the T_g of all of the polymers (unlike high temperature poling), this also allows an observation of the residual stable birefringence that remains in the samples after the orienting laser light is removed. A typical photoinduced birefringence writing curve (that of a PAC-5 film) is displayed in Figure 2, where linearly polarized light is introduced to the thin film at time $t = 10$ s to induce birefringence, and removed at time $t = 60$ s. At time $t = 370$ s, circularly polarized light of the same wavelength is introduced to erase the birefringence. At time $t = 60$ s when the writing laser is removed, there is a relaxation from the saturation level of birefringence on the order of hundreds of seconds, and the orientation that remains after this time is stable temporally until the introduction of circularly polarized light at time $t = 370$ s or until the sample is heated to T_g.

The maximum levels of birefringence which could be induced in each sample in the series are listed in Table 1. From previous studies of photoinduced birefringence in similar azobenzene polymers,[22,23] it has been shown that the growth section of the curve depicted in Figure 2 can be modeled effectively with a biexponential equation

$$\Delta n/\Delta n_{max} = A(1 - \exp(-t/t_a)) + B(1 - \exp(-t/t_b)) \tag{1}$$

where A and B are normalized constants ($A + B = 1$) describing the relative contributions of two exponential growth functions described by characteristic time constants t_a and t_b. If $t_a < t_b$, then these can be regarded as the time constants for a fast and slow growth rate respectively, with a fast rate coefficient A and a slow rate coefficient B. Similarly, the relaxation section of the birefringence curves depicted in Figure 2 can be closely approximated with a biexponential decay equation

$$\Delta n/\Delta n_{max} = C\exp(-t/t_c) + D\exp(-t/t_d) + E \tag{2}$$

where C and D are coefficients describing the fast and slow exponential relaxations with characteristic time constants of t_c and t_d when $t_c < t_d$.[22,23] E represents the fraction of the induced birefringence which is stable over

**Table 2. Time Constants and Coefficients Obtained from Curve Fitting**

n	A	t_a (s)	B	t_b (s)	C	t_c (s)	D	t_d (s)	E
2	0.87	0.78	0.13	7.77	0.06	4.28	0.16	205	0.78
3	0.92	0.65	0.08	6.40	0.05	5.11	0.15	202	0.80
4	0.92	0.77	0.08	11.0	0.10	3.41	0.19	168	0.72
5	0.92	0.67	0.08	9.00	0.08	3.80	0.17	153	0.75
6	0.93	0.63	0.07	8.42	0.09	3.84	0.22	157	0.69
8	0.95	0.50	0.05	7.77	0.11	3.77	0.25	153	0.64
9	0.95	0.57	0.05	15.8	0.12	3.56	0.26	136	0.62
10	0.97	0.47	0.03	35.6	0.16	2.63	0.29	131	0.55

time, and C, D, and E are also normalized. Using eqs 1 and 2, both the growth and the relaxation curves for all samples were fit to determine the dimensionless coefficients A, B, C, D, and E; and the characteristic time constants t_a, t_b, t_c, and t_d in seconds. The fitted biexponential curves lay within the experimental noise recorded by the probe beam detection equipment, and results of this curve fitting are presented in Table 2. Error estimates for the fits of the data to eqs 1 and 2 were observed to be similar to those presented in previous curve-fitting publications.[22,23]

From examination of these component coefficients, it is obvious that the orientation process is dominated by one time constant, that of the fast process. In the relaxation process both the fast and the slow components make an appreciable contribution, though that of the slower component is dominant. From the values of t_a and t_d, it is clear that there is a definite trend toward a shorter time constant (and hence a faster process) for both the growth and relaxation components, by nearly 50% in both cases, as the spacer length in the polymers is increased from 2 to 10 methylene units. This can be attributed to the increased mobility of the side chains, as both of these processes involve substantial motion of the pendant chromophores within the bulk polymer matrix.

This trend is also apparent when one examines the levels of birefringence which can be induced at saturation (maximum Δn), and that which remains after relaxation (E). It is apparent that in addition to a faster rate, the levels of maximum and stable birefringence decrease significantly over the series as well. A strong suggestion that this dependence is due mainly to a mobility-enhancement and T_g depression becomes evident when the Δn and E data are plotted against ($T - T_g$), the difference between the experimental temperature and the glass transition temperature for each sample. These Δn vs ΔT plots are presented in Figures 3 and 4. The experimental uncertainty for the Δn measurements was ±10%.

What is useful to note from this treatment of the data is that the shape of the maximum and stable birefringence vs ΔT curves bears a resemblance to induced-order vs T plots for single-poled polymer samples over a range of temperatures which have been fit to a master curve of orientational decay.[24] Although this master curve describes the isothermal relaxation rate of poled order, and the observations here plotted here are of birefringence over temperature, the results are similar with respect to the general shape: as T_g is approached there is a sharp decrease in the orientation toward zero, as the equilibrium between the induced order and the thermal disorder is shifted toward disordering with increasing kT. This suggests that the maximum and stable levels of birefringence for the PAC-n series might all lie on a similar master curve and exhibit similar
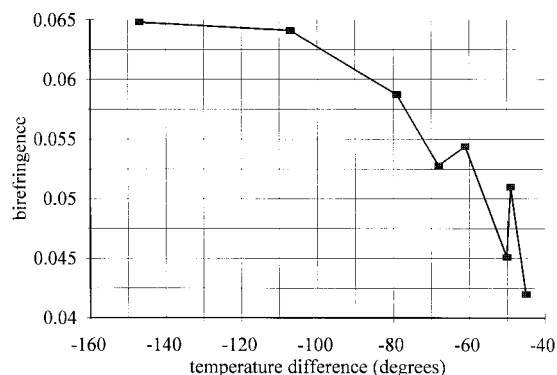
Figure 3. Maximum level of birefringence photoinducible vs $T - T_g$.
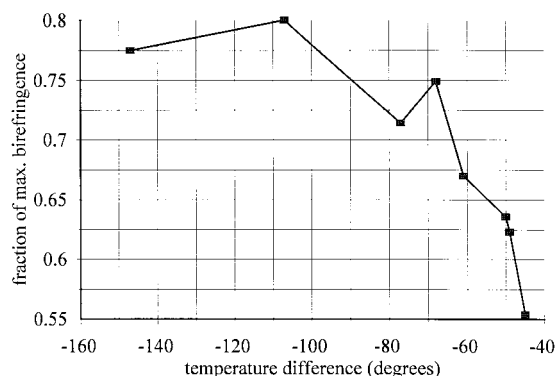
Figure 4. Fraction of photoinduced birefringence remaining after relaxation vs $T - T_g$.

behavior, once corrected for this temperature difference. This is further supported by the observation that when the electric field poling was carried out on the PAC-n samples "temperature corrected" to $T_g + 20$ °C, there was not a significant variation in rate or extent across the series. From these results it is clear that while orientation is more readily induced in polymers with a lower T_g, this advantage is overcome by the associated increase in thermal relaxation. The net effect of this appears to be that materials with the lowest mobility (those with the highest T_g) possess the potential for both the highest level of order which can be photoinduced and the greatest retention (lowest fraction of relaxation) of this induced order.

The photoconductivity (Φ in A/V·cm) of the polymer thin films was determined as described for all of the PAC-n polymers, and results are presented in Table 1. Although not as pronounced a trend as that of the induced birefringence, the data are consistent with a decrease in the photoconductivity over the series as the spacer length is increased. The experimental uncertainty in these measurements is equal to $\pm 2.5 \times 10^{-14}$ A/V·cm. As discussed, there is likely a decrease in the chromophore density across the series, and hence a comparison between the samples corrected for film thickness might not be as meaningful as a comparison correcting for the effective optical path length to account for chromophore dilution. This dilution effect would amount to ~20% across the series, however, in comparison to a ~30% decrease in Φ from the PAC-2 to the PAC-10 polymers.

After the samples are cast into EO cells and poled, photorefractive gratings can be inscribed by the method described. Films of these azobenzene polymers have been shown to be suitable materials for inscription of a
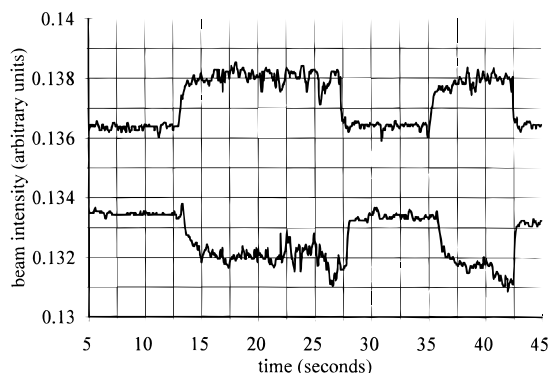
Figure 5. Change in beam intensity to demonstrate asymmetric two beam coupling in a PAC-5 photorefractive grating: top, intensity of beam 1; bottom, intensity of beam 2, as the other beam in introduced and removed.

Figure 6. Optical gain acheivable for the PAC-*n* photorefractive polymers.

variety of holographic gratings (such as isomerization, birefringence, and surface relief),[5,6] so four-wave mixing experiments to measure the photorefractive effect by diffraction efficiency would not be conclusive. Two-beam optical gain coupling at 633 nm was used to probe the formation of the photorefractive gratings, as it can be the only source of such an effect. While the λ_{max} of these polymers is in the UV and blue−visible range, there is still an appreciable absorption tail at 633 nm where measurements are taken. It was observed that this absorption by the gratings serves to reorient the poled chromophores by a weak isomerization and photoorientation mechanism, (especially at the high light intensities necessary for an appreciable photoconductive response), and erases the gratings with a time scale of minutes. Hence for these experiments two-beam coupling (2BC) was performed directly after poling, and the gain was recorded directly after PR grating inscription so as to minimize this erasure by the probe beam, and to compare effectively samples which display varying rates of poled order decay at room temperature. A typical 2BC optical gain experiment is depicted in Figure 5 for a PAC-5 EO cell.

The low signal-to-noise ratio illustrates that measurements at lower poling fields, lower irradiation intensities, or during relaxation could not easily be made, and the 15 V/μm poling field used for all samples represents the highest electric field that could be presented to the material before dielectric breakdown.

The two baselines represent the intensities of the two writing beams over the course of two consecutive experiments. The upper trace depicts the intensity of the first beam, and the lower trace the intensity of the second. With the first beam on, at time $t = 13$ s the other beam is introduced, and removed at time $t = 27$ s. The amount of increase (optical gain) of intensity of this beam is at the expense of a decrease (optical loss) in the other, and the optical gain can be estimated from this as 0.026 μm^{-1}. As there are other possible mechanisms for producing optical gain,[20] the amount of loss of the second beam (0.022 μm^{-1}) is used as an unambiguous measure of the PR gain of the first, since photorefractivity is the only mechanism that could be responsible for the asymmetric loss in these systems.[7] Non-PR gain during 2BC can arise from a variety of sources, including scattering of the second beam into the detector of the first beam, or increasing the transmittance of the sample by altering the cis/trans isomeric ratio in the photostationary state.[20] The loss observed
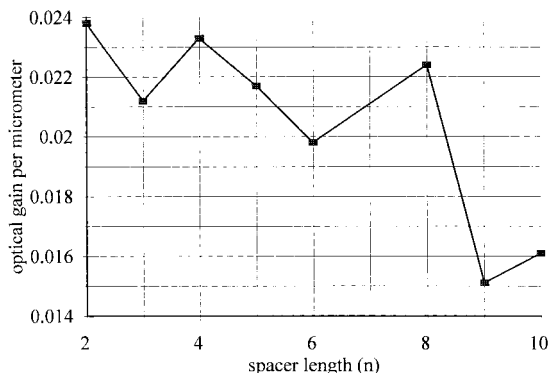
in these gratings was always of a lesser magnitude than the gain, so it is likely that some of these other non-PR gain effects are occurring simultaneously in these films. Two-beam coupling gain was not observed with unpoled samples, or with PR gratings that had been erased by high-intensity exposure at 633 nm for 30 min. In this fashion, the 2BC optical gain was determined for all PAC-*n* samples, and the results are presented in Figure 6. Although the magnitude of the experimental uncertainty ($\pm 30\%$) precludes a clear trend to be discerned, it appears that the samples with the longer spacers suffer a decrease in optical gain. This could be due to the photoconductivity decrease with increasing n as shown by the Φ values in Table 1, and it could also represent a decreased EO effect in addition to decreased charge transfer, as the higher n samples near T_g would likely suffer a greater loss of poled order due to relaxation and hence a decreased EO response. It is also possible that a mobility-dependent orientational enhancement of the optical gain is being observed.

While the carbazole/azobenzene-functionalized polymers possess a number of advantages as photorefractive materials such as high component concentration, sensitizer-free charge generation, internal field generated EO response, and versatility such as the potential for optically assisted poling, these materials also present a number of disadvantages to their application as PR holographic polymers. Foremost, the gain would have to be increased in order to exceed losses due to the strong optical absorption tail extending deep into the red ($\epsilon_{633} > 2200$ cm^{-1}) for net gain to be realized with two-beam coupling. This absorption loss of 0.2 μm^{-1} is still an order of magnitude above the 2BC gain observed here of ~0.02 μm^{-1}, so that at present no net gain is possible. This absorption also limits the thickness of the samples optically to a maximum of tens of micrometers when irradiating with light at 633 nm, which is still an order of magnitude thinner than any PR polymers which have been shown to produce a "useful" gain of >100% or more,[25] and this absorption appears to erase the grating during the reading process by a weak isomerization and subsequent photoorientation process. The two-beam coupling results do demonstrate however that the T_g of single-component multifunctional photorefractive polymers can be tailored over a range greater than 100°, without a significant change in the photorefractive effect.

Conclusions

A series of amorphous single-component multifunctional azocarbazole polymers in which the electrooptic

side chains are attached to a methacrylate backbone by spacers of various lengths was prepared and characterized, and substantial differences were observed in the rates and extent of photoinduced birefringence and orientational relaxation between the smaples. Polymers of the highest T_g displayed both the highest level of order which could be induced and the greatest fraction of this order that could be retained after orientational relaxation. A photorefractive two-beam optical gain of $0.024 \ \mu\text{m}^{-1}$ was demonstrated in films of the polymer with the highest glass transition temperature, although this was exceeded by absorption losses of the polymer, so that no net gain could be recorded at 633 nm.

References and Notes

(1) Rochon, P.; Gosselin, J.; Natansohn, A.; Xie, S. *Appl. Phys. Lett.* **1992**, *60*, 4.

(2) Sekkat, Z.; Wood, J.; Knoll, W. *J. Phys. Chem.* **1995**, *99*, 17226.

(3) Shi, Y.; Steier, W.; Yu, L.; Chen, M.; Dalton, L. *Appl. Phys. Lett.* **1991**, *59*, 2935.

(4) Barrett, C.; Natansohn, A.; Rochon, P.; Callender, C. L.; Robitaille, L. *Proc. SPIE* **1997**, *3006*, 441.

(5) Rochon, P.; Batalla, E.; Natansohn, A. *Appl. Phys. Lett.* **1995**, *66*, 136.

(6) Kim, D.; Tripathy, S.; Li, L.; Kumar, J. *Appl. Phys. Lett.* **1995**, *66*, 1166.

(7) Moerner, W.; Silence, S. *Chem. Rev.* **1994**, *94*, 127.

(8) Yu, L.; Chan, W.; Peng, Z.; Gharavi, A. *Acc. Chem. Res.* **1996**, *29*, 13.

(9) Zhang, Y.; Burzynski, R.; Ghosal, S.; Casstevens, M. *Adv. Mater.* **1996**, *8*, 111.

(10) Meerholz, K.; Volodin, B. L.; Sandalphon; Kippelen, B.; Peyghambarian, N. *Nature* **1994**, *371*, 497.

(11) Orczyk, M.; Zieba, J.; Prasad, P. *J. Phys. Chem.* **1994**, *98*, 8699.

(12) Silence, S.; Twieg, R.; Bjorklund, G.; Moerner, W. *Phys. Rev. Lett.* **1994**, *73*, 2047.

(13) Zhao, C.; Park, C.; Prasad, P.; Zhang, Y.; Ghosel, S.; Burzynski, R. *Chem. Mater.* **1995**, *7*, 1237.

(14) Zhang, Y.; Ghosal, S.; Casstevens, M.; Burzynski, R. *Appl. Phys. Lett.* **1995**, *66*, 256.

(15) Lundquist, P.; Wortmann, R.; Geletneky, C.; Twieg, R.; Jurich, M.; Lee, V.; Moylan, C.; Burland, D. *Science* **1996**, *274*, 1182.

(16) Zhang, Y.; Wang, L.; Wada, T.; Sasabe, H. *Appl. Phys. Lett.* **1997**, *70*, 2949.

(17) Ho, M.; Barrett, C.; Paterson, J.; Esteghamatian, M.; Natansohn, A.; Rochon, P. *Macromolecules* **1996**, *29*, 4613.

(18) Zhang, Y.; Wada, T.; Wang, L.; Aoyama, T.; Sasabe, H. *Chem. Commun.* **1996**, 2325.

(19) Schildkraut, J. *Appl. Phys. Lett.* **1991**, *58*, 340.

(20) Darracq, B.; Canva, M.; Chaput, F.; Boilot, J.; Riehl, D.; Lévy, Y.; Brun, A. *Appl. Phys. Lett.* **1997**, *70*, 292.

(21) Zobel, O.; Eckl, M.; Strohriegl, P.; Haarer, D. *Adv. Mater.* **1995**, *7*, 911.

(22) Ho, M.; Natansohn, A.; Barrett, C.; Rochon, P. *Can. J. Chem.* **1995**, *73*, 1773.

(23) Ho, M.; Natansohn, A.; Rochon, P. *Macromolecules* **1995**, *28*, 6124.

(24) Burland, D. M.; Miller, R. D.; Walsh, C. A. *Chem. Rev.* **1994**, *94*, 31.

(25) Grunnet-Jepsen, A.; Thompson, C.; Moerner, W. *Science* **1997**, *277*, 549.